

BLISS: A LIGHTWEIGHT BILEVEL INFLUENCE SCORING METHOD FOR DATA SELECTION IN LANGUAGE MODEL PRETRAINING

Anonymous authors

Paper under double-blind review

ABSTRACT

Effective data selection is essential for pretraining large language models (LLMs), enhancing efficiency and improving generalization to downstream tasks. However, existing approaches often require leveraging external pretrained models, making it difficult to disentangle the effects of data selection from those of the external pretrained models. In addition, they often overlook the long-term impact of selected data if the model is trained [for a long period of time](#), primarily due to the prohibitive cost of full-scale LLM pretraining. In this paper, we introduce **BLISS** (**Bilevel Influence Scoring** method for data **S**election): a lightweight data selection method that operates entirely *from scratch*, without relying on any external pretrained oracle models, while explicitly accounting for the long-term impact of selected data. BLISS leverages a small proxy model as a surrogate for the LLM and employs a score model to estimate the long-term influence of training samples if the proxy model is trained to convergence. We formulate data selection as a bilevel optimization problem, where the upper-level objective optimizes the score model to assign importance weights to training samples, ensuring that minimizing the lower-level objective (i.e., training the proxy model over the weighted training loss until convergence) leads to best validation performance. Once optimized, the trained score model predicts influence scores for the dataset, enabling efficient selection of high-quality samples for LLM pretraining. We validate BLISS by pretraining 410M/1B/2.8B Pythia and LLaMA-0.5B models on selected subsets of the C4 dataset. Notably, under the 1B model setting, BLISS achieves $1.7 \times$ speedup in reaching the same performance as the state-of-the-art method, demonstrating superior performance across multiple downstream tasks.

1 INTRODUCTION

The successful large-scale language model pretraining crucially relies on the careful choice of pretraining data (Brown et al., 2020; Raffel et al., 2020; Du et al., 2022; Elazar et al., 2023). Recent studies have shown that effective data selection (a.k.a., data curation) methods can enhance pretraining efficiency (Xie et al., 2023a) and improve generalization (Engstrom et al., 2024; Wettig et al., 2024). There are various types of data selection approaches for language model pretraining, including language filtering (Laurençon et al., 2022; Wenzek et al., 2019), data deduplication (Lee et al., 2021; Abbas et al., 2023), heuristic approaches (Rae et al., 2021; Penedo et al., 2023), data quality data filtering (Brown et al., 2020; Gao et al., 2020; Chowdhery et al., 2023; Xie et al., 2023b; Wettig et al., 2024), data mixing (Xie et al., 2023a; Albalak et al., 2023; Xia et al., 2023), and data influence function based methods (Park et al., 2023; Engstrom et al., 2024; Yu et al., 2024). Despite the rich literature of data selection methods in large language model (LLM) pretraining (e.g., a survey paper in Albalak et al. (2024)), it is still unclear what properties are needed for the training data curation to guarantee good performance: it remains an important real-world challenge (Li et al., 2024).

Existing approaches of data selection methods suffer from two major limitations. First, they often require leveraging pretrained models (Brown et al., 2020; Xie et al., 2023b; Wettig et al., 2024) for data-quality filtering, making it difficult to separate the effects of data selection from those of the external pretrained models. For example, the QuRating method (Wettig et al., 2024) assigns quality ratings to training samples based on responses from a pretrained LLM (e.g., GPT-3.5) before training a QuRater model. This reliance raises uncertainty about the role of the external LLM in the training process and whether its feedback is truly optimal. Moreover, the cost of invoking these external pretrained models is prohibitively expensive during data selection process for large-scale pretraining.

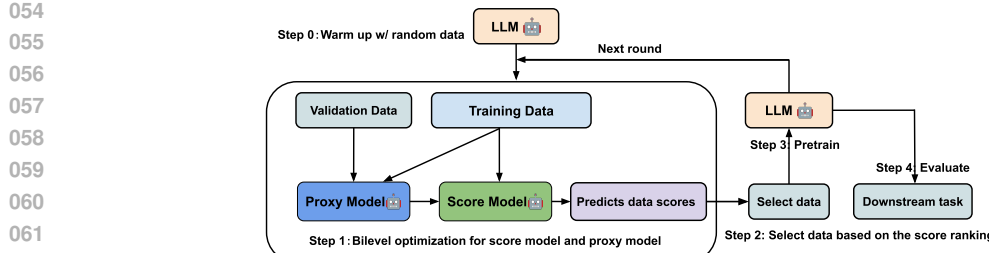


Figure 1: The pipeline of data selection and pretraining procedure. There are four main steps in one round training, 1) Warm up LLM using randomly selected training data (e.g. 10k step); 2) Bilevel optimization for score and proxy model, 3) Predict the data influence, and select Top-20% training data based on their score ranking; 4) Retrain the LLM using the selected data (e.g., 10k steps); 5) Evaluate on the downstream task. Repeating the above steps can achieve multiple-round training.

Second, they typically do not consider the long-term impact of selected data if the model is trained for a long time (i.e., multiple steps of gradient-based updates). For example, the data influence function based approach (Yu et al., 2024) evaluates the impact of individual training samples based on a single training step with the current model, which does not capture the cumulative effects of data selection over the course of full model training.

In this paper, we introduce a new data selection method, to address the two major limitations of existing approaches. Our method, namely **BLISS** (**Bilevel Influence Scoring** method for data Selection), is a lightweight data selection method that operates entirely *from scratch*, without relying on any external pretrained models, while explicitly accounting for the long-term impact of selected data. The core innovation of our approach lies in *the integration of two lightweight models within a novel bilevel optimization framework* for data selection. Our method bypasses traditional data-quality filtering and explicitly considers the long-term impact of selected data throughout training. In particular, BLISS leverages a small proxy model as a surrogate for the LLM and employs a score model to estimate the long-term influence of training samples if the proxy model is trained to convergence. Our bilevel optimization problem has upper-level and lower-level objectives: the upper-level objective optimizes the score model to assign importance weights to training samples, ensuring that minimizing the lower-level objective (i.e., training the proxy model over the weighted training loss until convergence) leads to best validation performance. Once the bilevel optimization is solved, the trained score model predicts influence scores for the entire dataset, enabling the selection of high-score samples for LLM pretraining. The pipeline of our proposed procedure is illustrated in Figure 1. The main contributions of our paper are summarized as the following:

- We propose a principled approach to data selection for language model pretraining. Our method, BLISS, leverages a novel bilevel optimization framework that employs a proxy model and a score model to explicitly account for the long-term impact of selected data. Unlike existing methods, BLISS operates from scratch without relying on any pretrained oracle models for data-quality filtering, obviating any biases or risks that may arise from such dependence¹.
- We validate our method by pretraining 410M/1B Pythia and LLaMA-0.5B models on selected subsets of C4 dataset. Experimental results on 1B setting demonstrate a $1.7 \times$ speedup in reaching the same performance as the state-of-the-art method such as MATES (Yu et al., 2024). Furthermore, we scale up our experiments to a 2.8B model pretraining used by the data selected in the 1B experiment, and we demonstrate that our method consistently outperforms MATES at every round of data selection, achieving 1.4% performance improvement over MATES (Yu et al., 2024).
- Through extensive ablation studies, we demonstrate the effectiveness of each component in our bilevel optimization framework, further substantiating the robustness and efficiency of our approach.

¹Many commercial large-scale pretrained models strictly prohibit users from generating data or using them to facilitate the training of other models, as doing so may result in severe legal consequences (OpenAI, 2024; Google, 2024). Our approach is entirely free from such legal concerns. We rely solely on algorithmic advancements applied to a model trained from scratch, without any dependence on third-party pretrained large-scale models.

108 **2 RELATED WORK**

109
110 **Data Selection for Language Model Training.** Early approaches to data selection primarily relied
111 on rule-based methods as language filters for training data, employing utility functions tailored to
112 specific datasets (Conneau & Lample, 2019; Raffel et al., 2020; Rae et al., 2021; Penedo et al.,
113 2023). Another key category is data deduplication (Lee et al., 2021; Sorscher et al., 2022; Penedo
114 et al., 2023; Abbas et al., 2023; Tirumala et al., 2023), which eliminates redundant samples to
115 optimize training efficiency and enhance performance on downstream tasks. A class of methods
116 exist for performing data-quality filtering, which can select data similar to high-quality corpus of
117 data points (Brown et al., 2020; Du et al., 2022; Gao et al., 2020; Xie et al., 2023b; Li et al., 2024),
118 with small perplexity (Chowdhery et al., 2023; Wenzek et al., 2019). More recent methods leverage
119 external pretrained LLMs to evaluate the pretraining data quality (Wettig et al., 2024; Maini et al.,
120 2024; Zhuang et al., 2025). In addition, a similar variant of data selection is domain reweighting for
121 data mixtures (Oren et al., 2019; Sagawa et al., 2019; Xie et al., 2023a; Fan et al., 2023; Albalak et al.,
122 2023; Chen et al., 2024), which re-scale the contribution of each domain to enhance generalization.
123 Another recently emerged line of research leverages the tool of influence functions (Hampel, 1974;
124 Cook, 1977; Ling, 1984; Koh & Liang, 2017) to evaluate the impact of individual training samples
125 on a fixed LLM (Park et al., 2023; Engstrom et al., 2024; Yu et al., 2024; Pan et al., 2025; Lin et al.,
126 2024). **QUAD (Zhang et al., 2024) proposes an efficient framework incorporating the attention layers**
127 **to estimate the influence scores.**

128 In contrast to these works, our work explicitly considers the long-term impact of selected data if the
129 model is not simply fixed but **trained for a long time**. In addition, our method can train the model
130 from scratch and does not need any extra information from any external pretrained models, making it
131 a scalable and effective solution.

132 **Bilevel Optimization and Data Selection.** Bilevel optimization provides a powerful framework
133 for modeling optimization problems with a nested structure (Bracken & McGill, 1973; Dempe,
134 2002). Recent research has focused on developing efficient bilevel optimization algorithms with
135 strong theoretical guarantees (Ghadimi & Wang, 2018; Hong et al., 2023; Ji et al., 2021; Kwon
136 et al., 2023; Dagréou et al., 2022; Chen et al., 2023; Grazzi et al., 2022; Hao et al., 2024; Gong
137 et al., 2024). This approach has been widely applied in various machine learning tasks, including
138 meta-learning (Finn et al., 2017), hyperparameter optimization (Franceschi et al., 2018), and natural
139 language processing (Somayajula et al., 2023; Grangier et al., 2023). For the application of data
140 selection, bilevel optimization has been utilized for continual learning (Borsos et al., 2020; Zhou et al.,
141 2022; Hao et al., 2023) and data reweighting in LLM fine-tuning (Pan et al., 2024; Shen et al., 2024).
142 Our work is most closely related to SEAL (Shen et al., 2024), which focuses on selecting high-quality
143 and safe data to fine-tune a pretrained LLM, with the goal of aligning the model with safety and
144 ethical guidelines. However, our approach differs from SEAL in two key aspects: (1) Problem setting.
145 While SEAL operates in a fine-tuning context, our objective is to select data for **pretraining** an
146 LLM from scratch, aiming to improve downstream performance **without relying on any external**
147 **pretrained models.** (2) Model update mechanism. SEAL utilizes the LoRA technique (Hu et al.,
148 2021) to update both the data selector and the LLM during fine-tuning. However, this approach is
149 not directly applicable to our setting due to the following reasons. First, LoRA is only suitable for
150 fine-tuning tasks but insufficient for full model pretraining. Second, their algorithm always updates
151 the original large models directly, which is computationally expensive if all parameters are updated.
152 In contrast, we propose a more efficient framework that introduces lightweight models (a score model
153 and a proxy model) to guide data selection, while allowing full parameter updates within these smaller
154 networks. To the best of our knowledge, our proposed bilevel influence scoring method is the first to
155 leverage bilevel optimization techniques for data selection in LLM pretraining.

156 **3 PRELIMINARIES AND NOTATIONS**

157 Suppose that we have a large-scale training dataset $\mathcal{D}_{tr} = \{\xi_i \mid 0 \leq i \leq N - 1\}$ and a downstream
158 task \mathcal{D}_{ds} . The goal is to select a subset of training set, namely $\mathcal{D}_s = \{\xi_j \mid 0 \leq j \leq Q - 1, Q \leq N\}$,
159 to pretrain a large language model with a specific training budget (e.g., limited FLOPs), such that the
160 model can achieve high performance on the downstream task \mathcal{D}_{ds} . Generally, the downstream data is
161 inaccessible during pretraining. Instead, we can use a validation data $\mathcal{D}_{val} = \{\zeta_i \mid 0 \leq i \leq M - 1\}$
162 to estimate the model's performance on \mathcal{D}_{ds} , because these two datasets often have similar data
163 distributions or share common domain knowledge. A small subset of training data $\tilde{\mathcal{D}}_{tr} \subset \mathcal{D}_{tr}$ is
164 uniformly sampled from \mathcal{D}_{tr} .

In bilevel optimization, $f(\cdot)$ and $g(\cdot)$ denote the upper-level (UL) and lower-level (LL) functions, respectively. Machine learning often requires solving stochastic optimization problems $f(\cdot) = \mathbb{E}_{\xi \sim \mathcal{D}_f}[F(\cdot; \xi)]$ and $g(\cdot) = \mathbb{E}_{\zeta \sim \mathcal{D}_g}[G(\cdot; \zeta)]$, where \mathcal{D}_f and \mathcal{D}_g are the underlying unknown data distribution for f and g , respectively. $F(\cdot; \xi)$ denotes the upper-level stochastic objective function and $G(\cdot; \zeta)$ is the lower-level stochastic objective function. Noisy observations of f and g can be collected by sampling from \mathcal{D}_f and \mathcal{D}_g .

4 METHODS

4.1 BILEVEL INFLUENCE SCORING FRAMEWORK

The goal of data selection is to optimize the performance of the LLM on downstream tasks by training it using an optimal subset of training data. However, directly searching for the optimal subset of training samples faces prohibitive costs due to the combinatorial nature of the problem and the high computational cost of estimating the performance of the LLM for every potential subset being evaluated.

To address the aforementioned computational challenge, our bilevel influence scoring framework uses a lightweight score model θ_s to predict the influence of every sample on the model’s performance for the downstream task. The optimized score model is then used to infer the influence score of training samples, enabling the selection of the subset with the highest influence, thus streamlining the process to search for the optimal training data. Instead of directly estimating the performance of LLM (parameterized by θ_{tr}) which is computationally expensive, our framework introduces a lightweight proxy model θ_p to approximate the behavior of the LLM. Note that the score model and the proxy model are both small models: they share a similar architecture and number of parameters. To ensure the data preferences of the proxy model align with those of the LLM, we apply knowledge distillation by minimizing the Kullback-Leibler (KL) divergence between the output logits of the proxy model and the LLM. We formulate the bilevel optimization for data selection as follows:

$$\begin{aligned} \min_{\theta_s} \Phi(\theta_s) &:= f(\theta_p^*(\theta_s)) := \mathbb{E}_{\zeta \sim \mathcal{D}_{\text{val}}} F(\theta_p^*(\theta_s); \zeta) && \text{(UL),} \\ \text{s.t. } \theta_p^*(\theta_s) &\in \arg \min_{\theta_p} g(\theta_p, \theta_s) := \mathbb{E}_{\xi \sim \mathcal{D}_{tr}} G(\theta_p, \theta_s; \xi) && \text{(LL).} \end{aligned} \quad (1)$$

where $\mathbb{E}_{\xi \sim \mathcal{D}_{tr}} G(\theta_p, \theta_s; \xi) = \sum_{i=0}^{N-1} P_i \mathcal{L}(\theta_p; \xi_i) + \gamma D_{KL}(\ell(\theta_p; \xi_i) \| \ell(\theta_{tr}; \xi_i)) + \lambda \|\theta_p\|^2$ and $P_i = \frac{e^{h(\theta_s; \xi_i)}}{\sum_{j=1}^N e^{h(\theta_s; \xi_j)}}$ represents the importance weight of sample i , and $h(\cdot) : \mathbb{R}^{d_x} \rightarrow (0, 1)$ is a function that maps a sample from \mathbb{R}^{d_x} to an influence score in the range $(0, 1)$. $\mathcal{L}(\cdot)$ and $F(\cdot)$ denote the loss functions for next token prediction, with a common choice being cross-entropy. The model’s output logits are represented by $\ell(\cdot)$. The KL divergence is defined as $D_{KL}(X \| Y) = \sum_i X_i \log(\frac{X_i}{Y_i})$. γ and λ are the regularization coefficients for the KL divergence and the weight decay terms, respectively.

BLISS evaluates the long-term influence of training samples if the proxy model is trained to its convergence state $\theta_p^*(\theta_s)$. Specifically, the lower-level trains the proxy model on the weighted training loss until convergence. This is notably different from other methods such as MATES (Yu et al., 2024), which trains a single step on the selected data from the current model state before evaluating sample influence. Consequently, MATES overlooks the long-term influence of training samples and may not fully capture the importance of data for downstream tasks. It is also worth noting that the bilevel data selection framework, described in formula (1), does not rely on any external pretrained models which are typically trained on large-scale natural language corpora. This independence makes BLISS a more self-contained approach to data selection, which also obviates any biases or risks associated with external pretrained models that may involve proprietary or sensitive data.

4.2 ALGORITHM FOR UPDATING THE PROXY MODEL AND SCORE MODEL

Now we design efficient algorithms for solving the bilevel problem (1). The lower-level problem aims to optimize the proxy model θ_p on the weighted training samples with the influence predicted by the score model. Note that we freeze the LLM (θ_{tr}) through the process of solving the bilevel optimization problem, as the LLM is used to infer the output logits. Therefore, we perform the

216 following update for the lower-level objective on a mini-batch of size \mathcal{B} :
 217

$$\begin{aligned} 218 \quad \theta_p^{t+1} &= \theta_p^t - \eta_1 \nabla_{\theta_p} \sum_{i=1}^{\mathcal{B}} G(\theta_p^t, \theta_s^t; \xi_i) \\ 219 \quad &= \theta_p^t - \eta_1 \sum_{i=1}^{\mathcal{B}} \left(P_i \nabla_{\theta_p} \mathcal{L}(\theta_p^t; \xi_i) + \gamma \sum_j \nabla_{\theta_p} \ell_j(\theta_p^t; \xi_i) \log \frac{\ell_j(\theta_p^t; \xi_i)}{\ell_j(\theta_{tr}^t; \xi_i)} + 2\lambda \theta_p^t \right), \\ 220 \quad & \\ 221 \quad & \\ 222 \quad & \\ 223 \quad & \end{aligned} \tag{2}$$

224 where $\ell_j(\cdot)$ denotes the j -th logit of the output. Note that the exact computation of P_i depends on all
 225 N samples, which is computationally infeasible. Therefore, we approximate P_i by replacing the full
 226 summation in the denominator with a partial summation over a smaller subset. This approximation
 227 is implemented in a distributed manner, significantly reducing the computational overhead. More
 228 details can be found in Appendix G. For the upper-level update, we take the derivative of $\Phi(\theta_s)$ with
 229 respect to θ_s by chain rule, which is known as the hypergradient:
 230

$$\nabla_{\theta_s} \Phi(\theta_s) = -\nabla_{\theta_s \theta_p}^2 g(\theta_p^*(\theta_s), \theta_s) \underbrace{[\nabla_{\theta_p}^2 g(\theta_p^*(\theta_s), \theta_s)]^{-1} \nabla_{\theta_p} f(\theta_p^*(\theta_s))}_{z}, \tag{3}$$

233 where z is the solution of the quadratic function $\min_z \frac{1}{2} z^T \nabla_{\theta_p}^2 g(\theta_p^*(\theta_s), \theta_s) z - z^T \nabla_{\theta_p} f(\theta_p^*(\theta_s))$. It
 234 can be solved by running a few steps of gradient descent in practice:
 235

$$z_{k+1}^t = z_k^t - \eta_2 (\nabla_{\theta_p}^2 g(\theta_p^t, \theta_s^t) z_k^t - \nabla_{\theta_p} f(\theta_p^t)), \tag{4}$$

236 where k is the number of gradient updates for updating z at a fixed iteration t of updating θ_s . We
 237 run 3 steps of gradient descent to solve z in our experiments. Note that Equation (4) computes the
 238 Hessian-Vector-Product (HVP) term $\nabla_{\theta_p}^2 g(\theta_p^t, \theta_s^t) z_k^t$ and thus avoids the computationally prohibitive
 239 operation of taking the inverse of the Hessian. The dimension of z is the same as that of the parameters
 240 of the lightweight proxy model. Therefore, the computation of HVP within the PyTorch framework is
 241 quite similar to that of gradient. In our implementation, we use the stochastic variants of Equation (3)
 242 and Equation (4) for updating the score model. In particular, the approximation of hypergradient at
 243 iteration t on the mini-batch \mathcal{B} is
 244

$$\nabla_{\theta_s} \widehat{\Phi}(\theta_s^t) = - \sum_{i=1}^{\mathcal{B}} P_i \nabla_{\theta_s} h(\theta_s^t; \xi_i) \nabla_{\theta_p} \mathcal{L}(\theta_p^t; \xi_i) z^t + \sum_{i=1}^{\mathcal{B}} P_i \sum_{j=1}^{\mathcal{B}} P_j \nabla_{\theta_s} h(\theta_s^t; \xi_j) \nabla_{\theta_p} \mathcal{L}(\theta_p^t; \xi_i) z^t. \tag{5}$$

245 Then the update for the upper-level variable (θ_s) is $\theta_s^{t+1} = \theta_s^t - \eta_3 \nabla_{\theta_s} \widehat{\Phi}(\theta_s^t)$. When the score model
 246 converges over T steps, reaching θ_s^T , it is then used to estimate the influence scores of the entire
 247 training dataset in the current round by: $S_i = h(\theta_s^T, \xi_i)$, $\forall \xi_i \in \mathcal{D}_{tr}$. Then the influence scores are
 248 collected: $\{S_i \mid 0 \leq i \leq |\mathcal{D}_{tr}|\}$, and the top-ranked samples with the highest influence scores are
 249 selected to construct \mathcal{D}_s , which is used to pretraining the LLM (θ_{tr}) .
 250

251 The detailed implementation of the algorithm is presented in Algorithm 1. In practice, we use Adam
 252 optimizer (Kingma & Ba, 2014) to update the upper-level variables, where we will update the Adam
 253 gradient with the calculated hypergradient. The pretraining process is conducted over R rounds.
 254 In each round, the algorithm performs data selection followed by LLM retraining. The training
 255 dataset is partitioned into R shards. The data selection in round r is conducted on \mathcal{D}_{tr}^r . The LLM
 256 resumes training from the previous round's checkpoint and updates to θ_{tr}^r at the end of the r -th round.
 257 Similarly, the score model also continues learning throughout the process, reaching θ_s^r at the r -th
 258 round. It is worth noting that the proxy model (θ_p^r) is reinitialized with the warm-up model at the
 259 beginning of each round. This prevents the model from overfitting to the previous round's training
 260 data and ensures it can better capture the evolving behavior of the LLM.
 261

262 4.3 WARM UP MODELS

263 The key distinction between our algorithm and other data selection methods (Brown et al., 2020; Xie
 264 et al., 2023b; Wettig et al., 2024) is that it operates independently of external pretrained models, avoiding
 265 biases from data selection influenced by such models. However, without leveraging pretrained
 266 knowledge, the proxy model, score model, and LLM tend to perform poorly in the initial phase due to
 267 random parameter initialization. To mitigate this issue, we incorporate a model warm-up step before
 268 data selection, similar to other data selection approaches (Yu et al., 2024; Xia et al., 2024), using
 269

270
271**Algorithm 1** BLISS

1: **Input:** $\eta_1, \eta_2, \eta_3, R, T, K, Q, \mathcal{D}_{tr}, \tilde{\mathcal{D}}_{tr}, \mathcal{D}_{val}$
2: **Initialize:** Warm up $\theta_p^{0,0}, \theta_s^{0,0}, \theta_{tr}^{0,0}$ using randomly selected training data.
3: **for** $r = 0, \dots, R - 1$ **do**
4: $\theta_p^{0,r} = \theta_p^{0,0}$ # reset proxy/score parameters for the new round
5: $\theta_s^{0,r} = \theta_s^{T,r-1}$ if $r > 1$ else $\theta_s^{0,0}$
6: $\theta_{tr}^{0,r} = \theta_{tr}^{Q,r-1}$ if $r > 1$ else $\theta_{tr}^{0,0}$
7: **for** $t = 0, \dots, T - 1$ **do**
8: Sample $\xi_t^r, \tilde{\xi}_t^r, \pi_t^r \leftarrow \tilde{\mathcal{D}}_{tr}^r$, and sample $\zeta_t \leftarrow \mathcal{D}_{val}$
9: $\theta_p^{t+1,r} = \theta_p^{t,r} - \eta_1 \nabla_{\theta_p} G(\theta_p^{t,r}, \theta_s^{t,r}; \xi_t^r)$ # LL: update the proxy model for lower-level
10: $z^{t+1,r} = \text{GDLS}(\eta_2, K, \nabla_{\theta_p} G(\theta_p^{t,r}, \theta_s^{t,r}; \tilde{\xi}_t^r), \nabla_{\theta_p} F(\theta_p^{t,r}, \theta_s^{t,r}; \zeta_t))$ # solve the linear system
11: $\theta_s^{t+1,r} = \text{Adam}(\theta_s^{t,r}, -\nabla_{\theta_s \theta_p}^2 G(\theta_p^{t+1,r}, \theta_s^{t,r}; \pi_t^r) z^{t+1,r}, \eta_3)^2$ # UL: update the score model
12: **end for**
13: Infer the influence score $\{S_i^r \mid 0 \leq i \leq |\mathcal{D}_{tr}^r| - 1\}$ on \mathcal{D}_{tr}^r using $\theta_s^{T,r}$
14: Sort $\{S_i^r\}$ in descending order and select the 20% data with the highest influence scores from \mathcal{D}_{tr}^r to form the selected data \mathcal{D}_s
15: **for** $\tau = 0, \dots, Q - 1$ **do**
16: Sample ξ_τ from \mathcal{D}_s .
17: $\theta_{tr}^{\tau+1,r} = \theta_{tr}^{\tau,r} - \eta_4 \nabla_{\theta_{tr}} \ell(\theta_{tr}^{\tau,r}; \xi_\tau)$ # pretrain the LLM
18: **end for**
19: **end for**

293
294**Algorithm 2** GDLS: Gradient Descent for the Linear System Solution

1: **Input:** $\eta, K, \nabla_{\theta_p} g(\theta_p), a$
2: **Initialize:** z_0
3: **for** $k = 0, \dots, K - 1$ **do**
4: $z_k = z_{k-1}$ if $k > 1$ else z_0
5: $z_{k+1} = z_k - \eta (\nabla_{\theta_p}^2 g(\theta_p) z_k - a)$
6: **end for**
7: Return z_K

302
303
304
305
306

randomly selected samples. The lightweight proxy and score models share token embedding layers and transformer blocks but differ in their final layers: the proxy model handles token generation, while the score model outputs influence scores for individual samples. Consequently, only the proxy model and the LLM require warm-up, while the score model can be initialized with the weights from proxy model directly.

307
308

5 EXPERIMENTS

309
310
311
312
313
314
315
316
317
318
319

In this section, we validate the proposed bilevel influence scoring framework for pretraining data selection. We apply the bilevel optimization algorithm to train a lightweight proxy model (θ_p) and a score model (θ_s) for data selection. We then pretrain a target LLM (θ_{tr}), specifically Pythia-410M/1B, from scratch on a selected subset of the large-scale C4 dataset (Raffel et al., 2020), which is designed for LLM pretraining. we then evaluate the pretrained LLM on multiple downstream tasks and compare its performance against several baseline methods, including Random selection, DSIR (Xie et al., 2023b), SemDeDup (Abbas et al., 2023), DsDm (Engstrom et al., 2024), LESS (Xia et al., 2024), QuRating (Wettig et al., 2024), and MATES (Yu et al., 2024). We furthermore scale up our experiment to 2.8B model pretraining and achieve 1.4% performance improvement over the state-of-the-art method. [The domain reweighting experiment is deferred to Appendix J.](#)

320
321
322
323

5.1 DATASET SETTINGS

Following the approach of DsDm (Engstrom et al., 2024), we perform data selection and pretraining using tokenized data. The procedure of BLISS is implemented for 5 rounds (i.e., $R = 5$), with the

²[Adam\(variable, gradient, lr\)](#) optimizer receives the current variable, its hypergradient and learning rate. Then it updates the first and second momentum, then returns the updated variable.

324 C4 dataset partitioned into five equal shards, denoted as $\{\mathcal{D}_{tr}^r \mid 0 \leq r \leq 4\}$. Each training round
 325 operates on a distinct data shard without replacement. In every round, we first uniformly sample a
 326 small proportion (0.1%) from \mathcal{D}_{tr}^r as the bilevel training set $\tilde{\mathcal{D}}_{tr}^r$ for updating the proxy model. We
 327 use LAMBADA (Paperno et al., 2016) as validation data for updating the score model. Other datasets,
 328 including ARC-E (Clark et al., 2018), SQuAD (Rajpurkar, 2016), and PIQA (Bisk et al., 2020), are
 329 evaluated in the ablation study (Appendix C.4).

330 To evaluate the performance of data selection algorithms, we run the pretraining model across 9
 331 downstream tasks, including SciQ (Welbl et al., 2017), ARC-E (Clark et al., 2018), ARC-C (Clark
 332 et al., 2018), LogiQA (Liu et al., 2020), OBQA (Mihaylov et al., 2018), BoolQ (Clark et al., 2019),
 333 HellaSwag (Zellers et al., 2019), PIQA (Bisk et al., 2020), and WinoGrande (Sakaguchi et al., 2021).
 334 These tasks cover a diverse range of reasoning and comprehension challenges, including question
 335 answering, logical inference, commonsense reasoning, and coreference resolution. Thus it requires
 336 models to demonstrate various capabilities, such as retrieving and applying scientific knowledge,
 337 understanding causal relationships, resolving ambiguities in natural language, and making informed
 338 choices among distractors. A good data selection algorithm is expected to select the "important" data
 339 that boost model performance across these downstream tasks.

340 5.2 MODEL SETTINGS

341 The target pretraining model, Pythia-410M/1B/2.8B, consists of 410 million, 1 billion or 2.5 billion
 342 trainable parameters. Both the proxy model and score model are based on Pythia-31M (for Pythia-
 343 410M) or Pythia-160M (for Pythia-1B), but they serve different purposes: the proxy model acts as a
 344 surrogate for the LLM and is trained for next-token prediction, while the score model functions as a
 345 regression model that maps individual samples to corresponding influence scores. Details of model
 346 settings are deferred to Appendix A. Notably, all models are trained from scratch using Gaussian
 347 initialization for model parameters. Additional experimental details, including hyperparameter
 348 choices, learning rate schedules, and distributed training strategies, are provided in Appendix E.

350 5.3 BILEVEL OPTIMIZATION FOR PROXY MODEL AND SCORE MODEL

351 In the Pythia-410M setting, the proxy model θ_p is updated with a "single-step" optimization per
 352 iteration (line 9 in Algorithm 1). However, when scaling up to larger models like Pythia-1B, we
 353 adopt a "multi-steps" update strategy for the proxy model to achieve a better lower-level solution. To
 354 demonstrate the effectiveness of bilevel optimization in training the proxy model and score model,
 355 we visualize the evolution of the training loss at during round 2 (Figure 6(a) in Appendix F) and round
 356 5 (Figure 6(b) in Appendix F). Since the first round uses randomly selected data to warm up the LLM,
 357 our data selection algorithm is employed from the second round onward.

358 Within each round, both losses exhibit a two-phase trend: they initially decrease rapidly before
 359 experiencing a slight increase. This behavior arises due to the composition of the lower-level objective
 360 function, which includes three terms: the weighted cross-entropy loss, the KL divergence loss, and a
 361 regularization term. In the first phase, the weighted cross-entropy loss dominates, decreasing as the
 362 proxy model is optimized. In the second phase, the KL divergence term becomes more influential.
 363 Since the LLM has not yet been trained on the current dataset \mathcal{D}_{tr}^r (it only performs inference in
 364 bilevel training), its predictions may be suboptimal. The KL divergence term encourages the proxy
 365 model to mimic the behavior of this "imperfect" LLM, leading to a slight performance degradation.
 366 However, this ensures that the proxy model's data preference aligns with that of the LLM, improving
 367 the relevance of the selected training data and ultimately boosting the LLM's downstream task
 368 performance. An ablation study on the effect of KL divergence loss is presented in Section 6.2.

369 From round 2 to round 5, the score model is continuously optimized, leading to more accurate sample
 370 weight assignments. This, in turn, enhances the proxy model's performance on the weighted training
 371 samples, further improving the quality of data selection.

372 5.4 EVALUATION RESULTS ON THE DOWNSTREAM TASKS

373 The LLM is continuously trained for 10,000 steps on the selected data in each round. After completing
 374 five rounds of training, we evaluate the zero-shot performance of Pythia-410M/1B on various
 375 downstream tasks and report the average accuracy along with the standard error for each dataset (see
 376 Table 1). Our algorithm consistently outperforms MATES and random selection methods across
 377 multiple tasks. For example on 410M setting, BLISS, compared with MATES, improves 2.4% on

378
 379
 380
 381 Table 1: Comparison of methods on zero-shot evaluation over multiple downstream datasets
 382 (410M/1B model, 25B tokens data). Best results are marked bold. The accuracy with standard
 383 error is reported based on the lm-evaluation-harness (Gao et al., 2021) implementation.
 384
 385

Methods (#FLOPs $\times 10^{19}$)	SciQ	ARC-E	ARC-C	LogiQA	OBQA	BoolQ	HellaSwag	PIQA	WinoGrande	Average
410M Setting: 410M model, 25B tokens										
Random (6.35)	64.1 (1.5)	40.2 (1.0)	25.6 (1.3)	24.7 (1.7)	29.4 (2.0)	58.9 (0.9)	39.7 (0.5)	67.1 (1.1)	50.6 (1.4)	44.5 (1.3)
MATES (8.11)	65.7 (1.5)	41.5 (1.0)	25.0 (1.3)	26.1 (1.7)	30.8 (2.1)	60.6 (0.9)	41.0 (0.5)	67.8 (1.1)	51.8 (1.4)	45.7 (1.4)
BLISS (8.08)	68.1 (1.5)	42.2 (1.0)	25.1 (1.3)	27.3 (1.7)	29.6 (2.0)	59.3 (0.9)	41.2 (0.5)	68.2 (1.1)	52.0 (1.4)	45.9 (1.4)
1B Setting: 1B model, 25B tokens										
Random (17.67)	65.8 (1.5)	43.7 (1.0)	25.6 (1.3)	27.5 (1.8)	31.8 (2.1)	60.2 (0.9)	43.8 (0.5)	68.9 (1.1)	50.7 (1.4)	46.4 (1.4)
MATES (19.97)	67.3 (1.5)	44.9 (1.0)	25.9 (1.3)	28.7 (1.8)	32.2 (2.1)	60.9 (0.9)	45.3 (0.5)	69.5 (1.1)	52.4 (1.4)	47.5 (1.4)
BLISS (8.08)	69.4 (1.5)	45.7 (1.0)	24.8 (1.3)	25.8 (1.7)	33.2 (2.1)	59.8 (0.9)	47.8 (0.5)	71.6 (1.1)	52.9 (1.4)	47.9 (1.3)

386
 387
 388
 389 Table 2: Average evaluation accuracy (15B tokens data) by pretraining 2.8B model with data
 390 selected from the 1B model experiment.

391
 392
 393 Table 3: Average evaluation accuracy of 3 rounds
 394 by pretraining Llama-0.5B model. Llama-134M
 395 is deployed as the proxy model in BLISS.

Methods	Round 1 (Random)	Round 2	Round 3
MATES	45.9 (1.3)	47.4 (1.3)	47.6 (1.3)
BLISS	45.2 (1.3)	47.6 (1.3)	49.0 (1.3)

Methods	Round 1 (Random)	Round 2	Round 3
MATES	43.12 (1.27)	44.53 (1.27)	45.01 (1.27)
BLISS	43.12 (1.27)	44.57 (1.27)	45.65 (1.27)

396 SciQ, 0.7% on ARC-E, 0.8% on LogiQA, 0.2% on HellaSwag, 0.4% on PIQA, 0.2% on WinoGrande,
 397 and 0.2% on average accuracy (see Table 8). Additionally, Figure 2 presents the evaluation results
 398 in relation to pretraining FLOPs and training steps. BLISS consistently outperforms other baseline
 399 methods throughout the entire five-round pretraining process (with 10k steps per round). In particular,
 400 our method on 1B setting achieves a 1.7 \times speedup in reaching the same performance as MATES,
 401 further validating the effectiveness of our data selection approach.

402 **Scaling Up to 2.8B Model Pretraining using the Data Selected by 160M/1B Experiment.** To
 403 further validate the selected data is of good quality regardless of model size, we pretrain a larger
 404 model of 2.8B parameters with data selected from the 1B model experiment with 160M proxy
 405 and score models. We run MATES and BLISS for 3 rounds (15B tokens). As shown in Table 2,
 406 BLISS consistently outperforms MATES across all data selection rounds, achieving 1.4% accuracy
 407 improvement over MATES in round 3.

408 **Generalize model architecture to LLaMA family.** We also explore LLaMA architecture models to
 409 validate the generalization of our method. Specifically, we use LLaMA-0.5B as the target pretraining
 410 model, and LLaMA-134M as the proxy model and score model. In each round, we first minimize
 411 the difference between the proxy model and the target model by training the proxy model toward a
 412 lower KL divergence. Then we periodically reset the proxy model to the initial state, in addition to
 413 resetting it at the beginning of each round. Table 3 presents the evaluation results compared with
 414 MATES, where BLISS exhibits strong data selection performance. At the round 3, our algorithm
 415 improves over MATES by 0.6%. More details are presented in Appendix B.

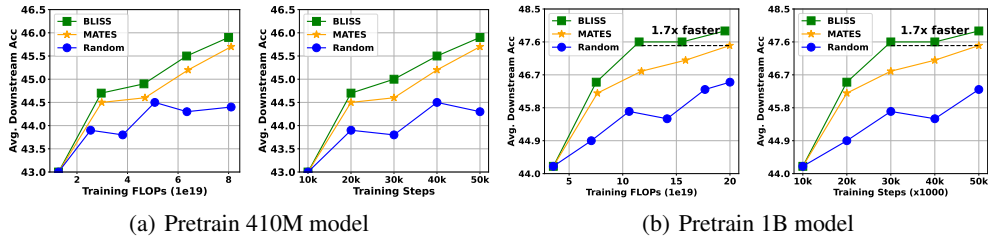
416 5.5 COMPUTATIONAL COST

417 We follows the FLOPs estimation method in Li et al. (2024) and report the total GPU FLOPs,
 418 including the pretraining, model warm-up, and data selection. Our main observation is: **without**
 419 **relying on any external pretrained models as required in MATES, BLISS achieves higher**
 420 **average downstream performance while consuming fewer FLOPs.** A detailed comparison of total
 421 FLOPs consumption is provided in Table 4, and running time/memory comparison is presented in
 422 Appendix H.

423 With the same pretraining budget for LLM and an equivalent number of training tokens, BLISS
 424 is more efficient in data selection than MATES. The higher computational cost of MATES is due
 425 to its reliance on oracle data influence estimation, which involves computing the loss change after
 426 performing a one-step gradient descent update on an individual training sample. This process is
 427 highly time-consuming, because it requires per-sample gradient and cannot increase the batch size
 428 per GPU. In contrast, BLISS formulates data selection as a bilevel optimization problem, enabling
 429 the lightweight score model and proxy model to be trained to convergence within relatively few
 430 steps, i.e., 3,000 per round (**ablation study for bilevel steps is presented in Appendix I**). While BLISS
 431 introduces additional training steps for warming up the proxy and score models from scratch, this
 432 cost is negligible compared to the overall pretraining FLOPs.

432
433 Table 4: Total FLOPs for pretraining 410M/1B model with 25B tokens.
434

Model	#FLOPs $\times 10^{19}$	Ratio	Model	#FLOPs $\times 10^{19}$	Ratio
MATES: 410M model, 25B tokens					
Model pretraining	6.35	78.3%	Model pretraining	6.35	79.28%
Oracle data influence collection	0.29	3.58%	Warm up the proxy/score model	0.07	0.87%
Data influence model training	0.01	0.1%	Bilevel optimization	0.13	1.62%
Data influence model inference	1.46	18.0%	Data influence model inference	1.53	19.10%
Total	8.11	100.00%	Total	8.08	100.00%
MATES: 1B model, 25B tokens					
Model pretraining	17.67	88.5%	Model pretraining	17.67	90.48%
Oracle data influence collection	0.83	4.1%	Warm up the proxy/score model	0.07	0.36%
Data influence model training	0.01	0.1%	Bilevel optimization	0.261	1.34%
Data influence model inference	1.46	7.3%	Data influence model inference	1.53	7.83%
Total	19.97	100.00%	Total	19.53	100.00%

442
443 Figure 2: The downstream performance of Pythia-410M/1B model w.r.t. pretraining FLOPs and
444 steps, where the first point denotes the performance of a warm-up model trained on random data.
445446

6 ABLATION STUDIES

447 To inspect the effectiveness of key techniques used in our proposed algorithm, we conduct ablation
448 studies on the effect of bilevel optimization (Section 6.1), KL divergence loss (Section 6.2), the
449 impact of softmax reparameterization on the score model’s outputs (Appendix C.1), the size of proxy
450 model (Appendix C.2), the initialization for the score model (Appendix C.3), and the influence of
451 different validation datasets (\mathcal{D}_{val}) on performance (Appendix C.4).
452453

6.1 SINGLE-LEVEL VERSUS BILEVEL OPTIMIZATION

454 In bilevel algorithm, the hyper-gradient is essential for the update of upper level parameters. To
455 verify the effectiveness of bilevel update for the upper-level parameters, we compare bilevel update
456 with a single update, which update θ_s and θ_p together using both training and validation data for the
457 lower-level objective. Specifically, the upper and lower levels are reduced to a single level problem:
458 the upper-level and lower-level parameters are updated simultaneously on validation dataset and
459 training dataset respectively. With the same number of training steps as bilevel training, the average
460 accuracy of single level update degrades 0.5% as shown in Table 5 in Appendix C.
461462

6.2 KL DIVERGENCE ALIGNS THE PROXY MODEL WITH THE LLM

463 Our objective is to select training data that maximizes the LLM’s performance on downstream tasks.
464 To achieve this, the proxy model must effectively represent the LLM, which we enforce by applying
465 KL divergence loss to align their output logits. As shown in Figure 3 (Appendix C), incorporating KL
466 divergence leads to improved performance across most downstream tasks, with a 9.3% accuracy boost
467 on LogiQA and a 1.4% increase in average accuracy. Interestingly, while removing KL divergence
468 results in a lower validation loss (as seen in Figure 7 compared to Figure 6(a) in Appendix F), it does
469 not translate to better downstream performance. These findings highlight the importance of bridging
470 the gap between the proxy model and the LLM to ensure effective data selection, demonstrating that
471 a closer alignment between the two models leads to better overall performance.
472473

7 CONCLUSION

474 In this paper, we present BLISS, a lightweight bilevel influence scoring method for data selection
475 in language model pretraining. BLISS utilizes a proxy model, a score model, and a novel bilevel
476 optimization framework to capture the long-term influence of data without relying on external
477 pretrained models. Experimental results demonstrate its effectiveness in selecting data for pretraining
478 Pythia and LLaMA models. However, current data selection methods primarily focus on language
479 models. In future work, we plan to extend our approach to visual or multimodal models.
480

486 REPRODUCIBILITY STATEMENT
487

488 We submit an anonymized code with training/evaluation scripts, configurations, seeds, and environment
489 files in the supplementary materials. All base models are publicly available: Pythia (under
490 EleutherAI Apache-2.0 license) and LLaMA (under Meta Llama 2 Community License Agreement).
491 Datasets C4 is accessible on HuggingFace under the licenses stated on their corresponding Hugging
492 Face dataset cards (loganengstrom/dsdm-candidate-c4). We include download scripts, preprocessing/
493 splits, and references to their dataset cards. These materials sufficiently support the reproduction
494 of our results.

495
496 REFERENCES
497

498 Amro Abbas, Kushal Tirumala, Dániel Simig, Surya Ganguli, and Ari S Morcos. Semdedup: Data-
499 efficient learning at web-scale through semantic deduplication. *arXiv preprint arXiv:2303.09540*,
500 2023.

501 Alon Albalak, Liangming Pan, Colin Raffel, and William Yang Wang. Efficient online data mixing
502 for language model pre-training. In *R0-FoMo: Robustness of Few-shot and Zero-shot Learning in*
503 *Large Foundation Models*, 2023.

504 Alon Albalak, Yanai Elazar, Sang Michael Xie, Shayne Longpre, Nathan Lambert, Xinyi Wang,
505 Niklas Muennighoff, Bairu Hou, Liangming Pan, Haewon Jeong, et al. A survey on data selection
506 for language models. *arXiv preprint arXiv:2402.16827*, 2024.

507 Yonatan Bisk, Rowan Zellers, Jianfeng Gao, Yejin Choi, et al. Piqa: Reasoning about physical
508 commonsense in natural language. In *Proceedings of the AAAI conference on artificial intelligence*,
509 volume 34, pp. 7432–7439, 2020.

510 Zalán Borsos, Mojmir Mutny, and Andreas Krause. Coresets via bilevel optimization for continual
511 learning and streaming. *Advances in Neural Information Processing Systems*, 33:14879–14890,
512 2020.

513 Jerome Bracken and James T McGill. Mathematical programs with optimization problems in the
514 constraints. *Operations Research*, 21(1):37–44, 1973.

515 Tom Brown, Benjamin Mann, Nick Ryder, Melanie Subbiah, Jared D Kaplan, Prafulla Dhariwal,
516 Arvind Neelakantan, Pranav Shyam, Girish Sastry, Amanda Askell, Sandhini Agarwal, Ariel
517 Herbert-Voss, Gretchen Krueger, Tom Henighan, Rewon Child, Aditya Ramesh, Daniel M. Ziegler,
518 Jeffrey Wu, Clemens Winter, Christopher Hesse, Mark Chen, Eric Sigler, Mateusz Litwin, Scott
519 Gray, Benjamin Chess, Jack Clark, Christopher Berner, Sam McCandlish, Alec Radford, Ilya
520 Sutskever, and Dario Amodei. Language models are few-shot learners. *Advances in neural*
521 *information processing systems*, 33:1877–1901, 2020.

522 Lesi Chen, Jing Xu, and Jingzhao Zhang. On bilevel optimization without lower-level strong
523 convexity. *arXiv preprint arXiv:2301.00712*, 2023.

524 Mayee Chen, Nicholas Roberts, Kush Bhatia, Jue Wang, Ce Zhang, Frederic Sala, and Christopher Ré.
525 Skill-it! a data-driven skills framework for understanding and training language models. *Advances*
526 *in Neural Information Processing Systems*, 36, 2024.

527 Aakanksha Chowdhery, Sharan Narang, Jacob Devlin, Maarten Bosma, Gaurav Mishra, Adam
528 Roberts, Paul Barham, Hyung Won Chung, Charles Sutton, Sebastian Gehrmann, et al. Palm:
529 Scaling language modeling with pathways. *Journal of Machine Learning Research*, 24(240):1–113,
2023.

530 Christopher Clark, Kenton Lee, Ming-Wei Chang, Tom Kwiatkowski, Michael Collins, and Kristina
531 Toutanova. Boolq: Exploring the surprising difficulty of natural yes/no questions. *arXiv preprint*
532 *arXiv:1905.10044*, 2019.

533 Peter Clark, Isaac Cowhey, Oren Etzioni, Tushar Khot, Ashish Sabharwal, Carissa Schoenick, and
534 Oyvind Tafjord. Think you have solved question answering? try arc, the ai2 reasoning challenge.
535 *arXiv preprint arXiv:1803.05457*, 2018.

540 Alexis Conneau and Guillaume Lample. Cross-lingual language model pretraining. *Advances in*
 541 *neural information processing systems*, 32, 2019.

542

543 R Dennis Cook. Detection of influential observation in linear regression. *Technometrics*, 19(1):15–18,
 544 1977.

545

546 Mathieu Dagréou, Pierre Ablin, Samuel Vaiter, and Thomas Moreau. A framework for bilevel
 547 optimization that enables stochastic and global variance reduction algorithms. *arXiv preprint*
 548 *arXiv:2201.13409*, 2022.

549

550 Stephan Dempe. *Foundations of bilevel programming*. Springer Science & Business Media, 2002.

551

552 DKYoon. Slimpajama-6b. HuggingFace Hub, 2023. <https://huggingface.co/datasets/DKYoon/SlimPajama-6B>.

553

554 Nan Du, Yanping Huang, Andrew M Dai, Simon Tong, Dmitry Lepikhin, Yuanzhong Xu, Maxim
 555 Krikun, Yanqi Zhou, Adams Wei Yu, Orhan Firat, et al. Glam: Efficient scaling of language
 556 models with mixture-of-experts. In *International Conference on Machine Learning*, pp. 5547–5569.
 557 PMLR, 2022.

558

559 Yanai Elazar, Akshita Bhagia, Ian Magnusson, Abhilasha Ravichander, Dustin Schwenk, Alane Suhr,
 560 Pete Walsh, Dirk Groeneweld, Luca Soldaini, Sameer Singh, et al. What’s in my big data? *arXiv*
 561 *preprint arXiv:2310.20707*, 2023.

562

563 Logan Engstrom, Axel Feldmann, and Aleksander Madry. Dsdm: Model-aware dataset selection
 564 with datamodels. *arXiv preprint arXiv:2401.12926*, 2024.

565

566 Simin Fan, Matteo Pagliardini, and Martin Jaggi. Doge: Domain reweighting with generalization
 567 estimation. *arXiv preprint arXiv:2310.15393*, 2023.

568

569 Chelsea Finn, Pieter Abbeel, and Sergey Levine. Model-agnostic meta-learning for fast adaptation of
 570 deep networks. In *International conference on machine learning*, pp. 1126–1135. PMLR, 2017.

571

572 Luca Franceschi, Paolo Frasconi, Saverio Salzo, Riccardo Grazzi, and Massimiliano Pontil. Bilevel
 573 programming for hyperparameter optimization and meta-learning. In *International Conference on*
 574 *Machine Learning*, pp. 1568–1577. PMLR, 2018.

575

576 Leo Gao, Stella Biderman, Sid Black, Laurence Golding, Travis Hoppe, Charles Foster, Jason Phang,
 577 Horace He, Anish Thite, Noa Nabeshima, Shawn Presser, and Connor Leahy. The pile: An 800gb
 578 dataset of diverse text for language modeling. *arXiv preprint arXiv:2101.00027*, 2020.

579

580 Leo Gao, Jonathan Tow, Stella Biderman, Sid Black, Anthony DiPofi, Charles Foster, Laurence
 581 Golding, Jeffrey Hsu, Kyle McDonell, Niklas Muennighoff, et al. A framework for few-shot
 582 language model evaluation. *Version v0. 0.1. Sept*, 10:8–9, 2021.

583

584 Saeed Ghadimi and Mengdi Wang. Approximation methods for bilevel programming. *arXiv preprint*
 585 *arXiv:1802.02246*, 2018.

586

587 Xiaochuan Gong, Jie Hao, and Mingrui Liu. A nearly optimal single loop algorithm for stochastic
 588 bilevel optimization under unbounded smoothness. In *Forty-first International Conference on*
 589 *Machine Learning*, 2024.

590

591 Google. Gemini API Additional Terms of Service, 2024. URL <https://ai.google.dev/gemini-api/terms>. Accessed: January 30, 2025.

592

593 David Grangier, Pierre Ablin, and Awni Hannun. Bilevel optimization to learn training distributions
 594 for language modeling under domain shift. In *NeurIPS 2023 Workshop on Distribution Shifts: New*
 595 *Frontiers with Foundation Models*, 2023.

596

597 Riccardo Grazzi, Massimiliano Pontil, and Saverio Salzo. Bilevel optimization with a lower-level
 598 contraction: Optimal sample complexity without warm-start. *arXiv preprint arXiv:2202.03397*,
 599 2022.

600

601 Frank R Hampel. The influence curve and its role in robust estimation. *Journal of the american*
 602 *statistical association*, 69(346):383–393, 1974.

594 Jie Hao, Kaiyi Ji, and Mingrui Liu. Bilevel coreset selection in continual learning: A new formulation
 595 and algorithm. *Advances in Neural Information Processing Systems*, 36, 2023.
 596

597 Jie Hao, Xiaochuan Gong, and Mingrui Liu. Bilevel optimization under unbounded smoothness: A
 598 new algorithm and convergence analysis. In *The Twelfth International Conference on Learning
 599 Representations*, 2024.

600 Mingyi Hong, Hoi-To Wai, Zhaoran Wang, and Zhuoran Yang. A two-timescale stochastic algorithm
 601 framework for bilevel optimization: Complexity analysis and application to actor-critic. *SIAM
 602 Journal on Optimization*, 33(1):147–180, 2023.
 603

604 Edward J Hu, Yelong Shen, Phillip Wallis, Zeyuan Allen-Zhu, Yuanzhi Li, Shean Wang, Lu Wang,
 605 and Weizhu Chen. Lora: Low-rank adaptation of large language models. *arXiv preprint
 606 arXiv:2106.09685*, 2021.

607 Kaiyi Ji, Junjie Yang, and Yingbin Liang. Bilevel optimization: Convergence analysis and enhanced
 608 design. In *International conference on machine learning*, pp. 4882–4892. PMLR, 2021.
 609

610 Diederik P Kingma and Jimmy Ba. Adam: A method for stochastic optimization. *International
 611 Conference on Learning Representations (ICLR)*, 2014.

612 Pang Wei Koh and Percy Liang. Understanding black-box predictions via influence functions. In
 613 *International conference on machine learning*, pp. 1885–1894. PMLR, 2017.
 614

615 Jeongyeol Kwon, Dohyun Kwon, Stephen Wright, and Robert D Nowak. A fully first-order method
 616 for stochastic bilevel optimization. In *International Conference on Machine Learning*, pp. 18083–
 617 18113. PMLR, 2023.

618 Hugo Laurençon, Lucile Saulnier, Thomas Wang, Christopher Akiki, Albert Villanova del Moral,
 619 Teven Le Scao, Leandro Von Werra, Chenghao Mou, Eduardo González Ponferrada, Huu Nguyen,
 620 et al. The bigscience roots corpus: A 1.6 tb composite multilingual dataset. *Advances in Neural
 621 Information Processing Systems*, 35:31809–31826, 2022.
 622

623 Katherine Lee, Daphne Ippolito, Andrew Nystrom, Chiyuan Zhang, Douglas Eck, Chris Callison-
 624 Burch, and Nicholas Carlini. Deduplicating training data makes language models better. *arXiv
 625 preprint arXiv:2107.06499*, 2021.

626 Jeffrey Li, Alex Fang, Georgios Smyrnis, Maor Ivgi, Matt Jordan, Samir Gadre, Hritik Bansal, Etash
 627 Guha, Sedrick Keh, Kushal Arora, et al. Datacomp-lm: In search of the next generation of training
 628 sets for language models. *arXiv preprint arXiv:2406.11794*, 2024.
 629

630 Huawei Lin, Jikai Long, Zhaozhuo Xu, and Weijie Zhao. Token-wise influential training data retrieval
 631 for large language models. *arXiv preprint arXiv:2405.11724*, 2024.

632 Robert F Ling. Residuals and influence in regression, 1984.
 633

634 Jian Liu, Leyang Cui, Hanmeng Liu, Dandan Huang, Yile Wang, and Yue Zhang. Logiqa: A
 635 challenge dataset for machine reading comprehension with logical reasoning. *arXiv preprint
 636 arXiv:2007.08124*, 2020.

637 Pratyush Maini, Skyler Seto, He Bai, David Grangier, Yizhe Zhang, and Navdeep Jaitly. Rephrasing
 638 the web: A recipe for compute and data-efficient language modeling. *arXiv preprint
 639 arXiv:2401.16380*, 2024.
 640

641 Todor Mihaylov, Peter Clark, Tushar Khot, and Ashish Sabharwal. Can a suit of armor conduct
 642 electricity? a new dataset for open book question answering. *arXiv preprint arXiv:1809.02789*,
 643 2018.

644 OpenAI. OpenAI Terms of Service, 2024. URL <https://openai.com/terms>. Accessed: Jan
 645 30, 2025.
 646

647 Yonatan Oren, Shiori Sagawa, Tatsunori B Hashimoto, and Percy Liang. Distributionally robust
 648 language modeling. *arXiv preprint arXiv:1909.02060*, 2019.

648 Rui Pan, Jipeng Zhang, Xingyuan Pan, Renjie Pi, Xiaoyu Wang, and Tong Zhang. Scalebio: Scalable
 649 bilevel optimization for llm data reweighting. *arXiv preprint arXiv:2406.19976*, 2024.
 650

651 Yanzhou Pan, Huawei Lin, Yide Ran, Jiamin Chen, Xiaodong Yu, Weijie Zhao, Denghui Zhang, and
 652 Zhaozhuo Xu. Alinfik: Learning to approximate linearized future influence kernel for scalable
 653 third-party llm data valuation. *arXiv preprint arXiv:2503.01052*, 2025.

654 Denis Paperno, Germán Kruszewski, Angeliki Lazaridou, Quan Ngoc Pham, Raffaella Bernardi,
 655 Sandro Pezzelle, Marco Baroni, Gemma Boleda, and Raquel Fernández. The lambada dataset:
 656 Word prediction requiring a broad discourse context. *arXiv preprint arXiv:1606.06031*, 2016.
 657

658 Sung Min Park, Kristian Georgiev, Andrew Ilyas, Guillaume Leclerc, and Aleksander Madry. Trak:
 659 Attributing model behavior at scale. *arXiv preprint arXiv:2303.14186*, 2023.

660 Guilherme Penedo, Quentin Malartic, Daniel Hesslow, Ruxandra Cojocaru, Alessandro Cappelli,
 661 Hamza Alobeidli, Baptiste Pannier, Ebtesam Almazrouei, and Julien Launay. The refinedweb
 662 dataset for falcon llm: outperforming curated corpora with web data, and web data only. *arXiv
 663 preprint arXiv:2306.01116*, 2023.

664 Jack W Rae, Sebastian Borgeaud, Trevor Cai, Katie Millican, Jordan Hoffmann, Francis Song, John
 665 Aslanides, Sarah Henderson, Roman Ring, Susannah Young, et al. Scaling language models:
 666 Methods, analysis & insights from training gopher. *arXiv preprint arXiv:2112.11446*, 2021.
 667

668 Colin Raffel, Noam Shazeer, Adam Roberts, Katherine Lee, Sharan Narang, Michael Matena, Yanqi
 669 Zhou, Wei Li, and Peter J Liu. Exploring the limits of transfer learning with a unified text-to-text
 670 transformer. *Journal of machine learning research*, 21(140):1–67, 2020.

671 P Rajpurkar. Squad: 100,000+ questions for machine comprehension of text. *arXiv preprint
 672 arXiv:1606.05250*, 2016.

673 Shiori Sagawa, Pang Wei Koh, Tatsunori B Hashimoto, and Percy Liang. Distributionally robust
 674 neural networks. In *International Conference on Learning Representations (ICLR)*, 2019.

675 Keisuke Sakaguchi, Ronan Le Bras, Chandra Bhagavatula, and Yejin Choi. Winogrande: An
 676 adversarial winograd schema challenge at scale. *Communications of the ACM*, 64(9):99–106,
 677 2021.

678 Han Shen, Pin-Yu Chen, Payel Das, and Tianyi Chen. Seal: Safety-enhanced aligned llm fine-tuning
 679 via bilevel data selection. *arXiv preprint arXiv:2410.07471*, 2024.

680 Sai Ashish Somayajula, Lifeng Jin, Linfeng Song, Haitao Mi, and Dong Yu. Bi-level finetuning with
 681 task-dependent similarity structure for low-resource training. In *Findings of the Association for
 682 Computational Linguistics: ACL 2023*, pp. 8569–8588, 2023.

683 Ben Sorscher, Robert Geirhos, Shashank Shekhar, Surya Ganguli, and Ari Morcos. Beyond neural
 684 scaling laws: beating power law scaling via data pruning. *Advances in Neural Information
 685 Processing Systems*, 35:19523–19536, 2022.

686 Kushal Tirumala, Daniel Simig, Armen Aghajanyan, and Ari Morcos. D4: Improving llm pretraining
 687 via document de-duplication and diversification. *Advances in Neural Information Processing
 688 Systems*, 36:53983–53995, 2023.

689 Johannes Welbl, Nelson F Liu, and Matt Gardner. Crowdsourcing multiple choice science questions.
 690 *arXiv preprint arXiv:1707.06209*, 2017.

691 Guillaume Wenzek, Marie-Anne Lachaux, Alexis Conneau, Vishrav Chaudhary, Francisco Guzmán,
 692 Armand Joulin, and Edouard Grave. Ccnet: Extracting high quality monolingual datasets from
 693 web crawl data. *arXiv preprint arXiv:1911.00359*, 2019.

694 Alexander Wettig, Aatmik Gupta, Saumya Malik, and Danqi Chen. Qurating: Selecting high-quality
 695 data for training language models. *arXiv preprint arXiv:2402.09739*, 2024.

696 Mengzhou Xia, Tianyu Gao, Zhiyuan Zeng, and Danqi Chen. Sheared llama: Accelerating language
 697 model pre-training via structured pruning. *arXiv preprint arXiv:2310.06694*, 2023.

702 Mengzhou Xia, Sadhika Malladi, Suchin Gururangan, Sanjeev Arora, and Danqi Chen. Less:
703 Selecting influential data for targeted instruction tuning. *arXiv preprint arXiv:2402.04333*, 2024.
704

705 Sang Michael Xie, Hieu Pham, Xuanyi Dong, Nan Du, Hanxiao Liu, Yifeng Lu, Percy Liang, Quoc V
706 Le, Tengyu Ma, and Adams Wei Yu. Doremi: Optimizing data mixtures speeds up language model
707 pretraining. *Advances in Neural Information Processing Systems*, 2023a.

708 Sang Michael Xie, Shibani Santurkar, Tengyu Ma, and Percy S Liang. Data selection for language
709 models via importance resampling. *Advances in Neural Information Processing Systems*, 36:
710 34201–34227, 2023b.

711 Zichun Yu, Spandan Das, and Chenyan Xiong. Mates: Model-aware data selection for efficient
712 pretraining with data influence models. *arXiv preprint arXiv:2406.06046*, 2024.

713 Rowan Zellers, Ari Holtzman, Yonatan Bisk, Ali Farhadi, and Yejin Choi. Hellaswag: Can a machine
714 really finish your sentence? *arXiv preprint arXiv:1905.07830*, 2019.

715 C Zhang, H Zhong, K Zhang, C Chai, R Wang, X Zhuang, T Bai, J Qiu, L Cao, J Fan, et al.
716 Harnessing diversity for important data selection in pretraining large language models. *arXiv
717 preprint arXiv:2409.16986*, 2024.

718 Xiao Zhou, Renjie Pi, Weizhong Zhang, Yong Lin, Zonghao Chen, and Tong Zhang. Probabilistic
719 bilevel coreset selection. In *International Conference on Machine Learning*, pp. 27287–27302.
720 PMLR, 2022.

721 Xinlin Zhuang, Jiahui Peng, Ren Ma, Yinfan Wang, Tianyi Bai, Xingjian Wei, Qiu Jiantao, Chi
722 Zhang, Ying Qian, and Conghui He. Meta-rater: A multi-dimensional data selection method for
723 pre-training language models. In *Proceedings of the 63rd Annual Meeting of the Association for
724 Computational Linguistics (Volume 1: Long Papers)*, pp. 10856–10896, 2025.

725

726

727

728

729

730

731

732

733

734

735

736

737

738

739

740

741

742

743

744

745

746

747

748

749

750

751

752

753

754

755

756 **A DETAILS OF MODEL SETTINGS**
757

758 The proxy model and score model serve different purposes: the proxy model acts as a surrogate
759 for the LLM and is trained for next-token prediction, while the score model functions as a re-
760 gression model that maps individual samples to their corresponding influence scores. To trans-
761 form the proxy model into the score model, we modify its architecture by replacing the final
762 Linear layer with an AdaptiveAvgPool layer, followed by a Linear layer and a Sigmoid
763 activation. Specifically, given the output from the preceding transformer blocks with dimension
764 [Batch, token_size, Emb_size], the AdaptiveAvgPool layer computes the average em-
765 bedding feature across tokens. The Linear layer then maps the pooled token representations to a
766 single-dimensional output, which is subsequently passed through a Sigmoid activation to produce
767 an influence score within the range (0, 1). In contrast, the proxy model’s final Linear layer maps
768 features from previous layers to the vocabulary dimension for token prediction.

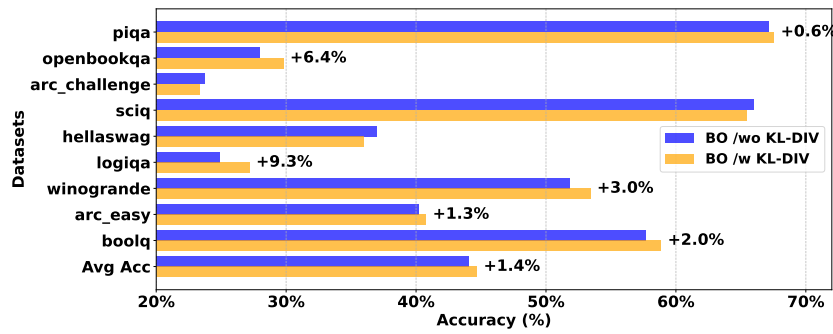
769 **B IMPLEMENTATION DETAILS IN LLaMA EXPERIMENT**
770

771 **Model Setup** In LLaMA setting, the target model is LLaMA-0.5B, and the proxy/score model is
772 LLaMA-134M. They are warmed up under the same process as Pythia setting.

773 **Training Details of Proxy/Score Model** There is a little difference in how we deal with the proxy
774 model in LLaMA setting compared to Pythia setting. In addition to resetting the proxy model
775 (LLaMA-134M) at the beginning of each round, we reset it to the initial state every 50 steps of the
776 update of the score model. We distill the target model into the proxy model by minimizing the KL
777 divergence for 240 steps. Then the checkpoint of the proxy model is saved as “initial” state. Since
778 periodic resetting the proxy model ensures a close alignment between two models, we remove the KL
779 divergence regulation term in the lower level loss function. To achieve a better lower-level solution,
780 the proxy model executes 4 lower-level updates, each computed on a batch of 64 samples. After the
781 score model is trained for 50 optimization steps, we reset the proxy model to the initial state.

782 **C MORE ABLATION STUDIES**
783

784 In this section, we provide more ablation studies to verify the effectiveness of each component in our
785 algorithm design.



800 Figure 3: The performance comparison of bilevel optimization with/without KL divergence. The
801 number on the bar indicate the accuracy improvement compared to the method without KL divergence.
802

803 Table 5: Comparison of BLISS with different settings (without softmax and single level update) over
804 multiple downstream datasets (410M model, 10B tokens) with 20k-step training.

Methods	SciQ	ARC-E	ARC-C	LogiQA	OBQA	BoolQ	HellaSwag	PIQA	WinoGrande	Average
Without softmax	63.5(1.5)	41.0(1.0)	22.4(1.2)	25.7(1.7)	30.0(2.1)	52.8(0.9)	38.8(0.5)	67.4(1.1)	51.0(1.4)	43.6(1.3)
Single Level	64.4(1.5)	42.3(1.0)	22.2(1.2)	24.1(1.7)	30.6(2.1)	55.0(0.9)	39.7(0.5)	67.1(1.1)	52.1(1.4)	44.2(1.3)
BLISS	65.5(1.5)	40.8(1.0)	23.4(1.2)	27.2(1.7)	29.8(2.0)	58.9(0.9)	36.0(0.5)	67.6(1.1)	53.4(1.4)	44.7(1.3)

810
811 Table 6: Comparison of BLISS with different size of proxy/score model and on zero-shot evaluation
812 over multiuple downstream datasets (410M model, 10B tokens) with 20k-step training.

Method	SciQ	ARC-E	ARC-C	LogiQA	OBQA	BoolQ	HellaSwag	PIQA	WinoGrande	Average
BLISS (Pythia-31M)	65.5(1.5)	40.8(1.0)	23.4(1.2)	27.2(1.7)	29.8(2.0)	58.9(0.9)	36.0(0.5)	67.6(1.1)	53.4(1.4)	44.7(1.3)
BLISS (Pythia-160M)	63.8(1.5)	40.8(1.0)	23.4(1.2)	27.5(1.8)	29.8(2.0)	51.3(0.9)	38.3(0.5)	67.6(1.1)	50.4(1.4)	44.1(1.3)

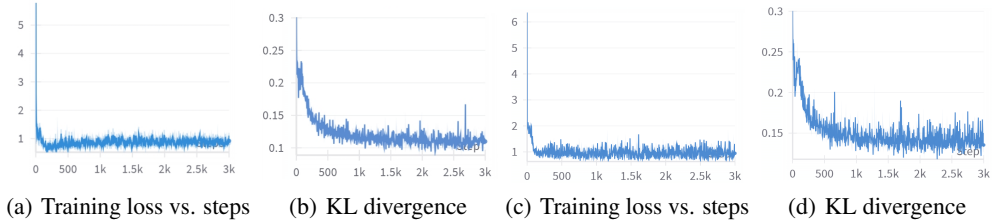
817 C.1 SOFTMAX REPARAMETRIZATION FOR SCORE MODEL'S OUTPUT

818
819 In our experiment, we apply a softmax function on all batch samples' score across GPUs to obtain
820 the importance weights P_i . Note that the raw output of the score model is already within the range
821 (0, 1), but we add another softmax function on top of it. We want to demonstrate the effectiveness of
822 this softmax reparameterization. Intuitively, the main benefit is that it naturally amplifies important
823 samples while downweighting less useful ones, improving the overall data selection process.

824 To assess the impact of the softmax reparameterization, we conduct an ablation experiment comparing
825 two approaches: (i) naive weighting, where the raw outputs of the score model are used directly
826 as sample weights; (ii) softmax weighting, where the softmax-transformed outputs of the score
827 model determine the sample weights. The results, shown in Table 5, indicate that softmax weighting
828 consistently outperforms naive weighting, leading to a 1.1% improvement in average downstream
829 accuracy. This demonstrates that softmax effectively enhances data selection by better distinguishing
830 important samples.

831 C.2 THE SIZE OF PROXY MODEL

832
833 We conduct experiments using two different sizes of proxy/score models (31M and 160M) for a
834 410M LLM. We observe that the KL divergence between the proxy and the LLM remains low for
835 both sizes-0.15 for the 160M model and 0.10 for the 31M model. The corresponding learning curves
836 are shown in Figure 4, which presents the results from round 2. The performance comparison of two
837 sizes of proxy model is summarized in Table 6. These findings suggest that even a small proxy model
838 (31M) is sufficient to serve as an effective surrogate for the 410M LLM.



839
840 Figure 4: The evolution of the lower-level training loss and KL divergence for different proxy model
841 size. Subfigures (a), (b): Proxy model size 31M, target LLM size 410M. Subfigures (c), (d): Proxy
842 model size 160M, target LLM size 410M.

843 C.3 INITIALIZATION METHOD FOR THE SCORE MODEL

844
845 In Algorithm 1, we initialize the score model in each new round using the parameters from the last
846 round. This design is motivated by the role of the score model: it learns data representations and ranks
847 the importance of training samples. As training progresses, the model's ability of feature learning
848 improves, making it beneficial to retain learned representations across rounds.

849 To validate this, we conduct ablation studies comparing two cases:

1. **Original BLISS (BLISS-org):** the score model in each round is initialized with the parameters from the last round.
2. **Modified Initialization (BLISS[†]):** the score model in each round is reset to its initial parameters from round 1.

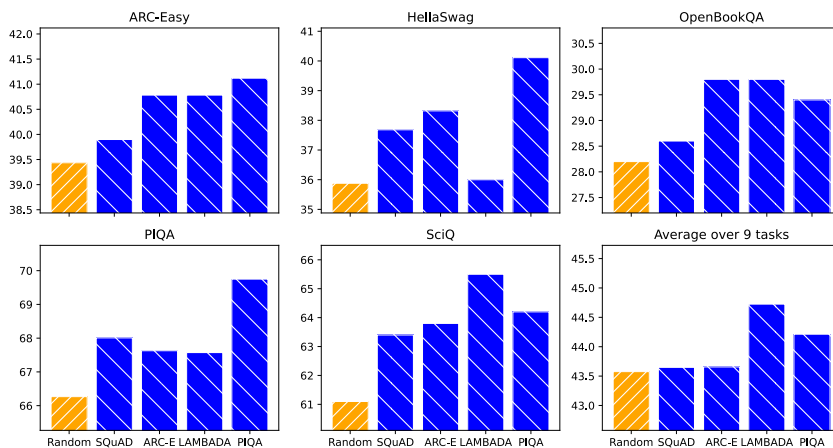


Figure 5: Comparison of BLISS trained with different validation datasets (410M model, 10B tokens). We compare our method with different validation datasets with random selection on 1 downstream task in each subplot.

We then use the trained score models from two cases to select training data and pretrain the target LLM for 15B tokens, respectively. The resulting LLMs are evaluated on multiple downstream datasets. As shown in Table 7, BLISS^\dagger achieves an average performance that is 0.4% lower than $\text{BLISS-}\text{org}$, demonstrating that continuous initialization leads to better data ranking and improved downstream performance.

Table 7: Comparison of methods on zero-shot evaluation over multiple downstream datasets (410M model, 15B tokens). $\text{BLISS-}\text{org}$ denotes the original algorithm, and BLISS^\dagger is a variant which uses different initialization method for the score model.

Methods (#FLOPs $\times 10^{19}$)	SciQ	ARC-E	ARC-C	LogiQA	OBQA	BoolQ	HellaSwag	PIQA	WinoGrande	Average
BLISS- org	67.7 (1.5)	41.7 (1.0)	23.6 (1.2)	25.8 (1.7)	28.4 (2.0)	56.0 (0.8)	39.7 (0.5)	68.7 (1.1)	53.2 (1.4)	44.9 (1.3)
BLISS †	65.2 (1.5)	41.6 (1.0)	23.4 (1.2)	27.1 (1.7)	29.8 (2.0)	57.5 (0.8)	34.9 (0.5)	67.7 (1.1)	53.5 (1.4)	44.5 (1.3)

C.4 VALIDATION DATASETS

The upper-level optimization aims to minimize the proxy model’s loss on the validation dataset, meaning different validation datasets influence data selection. We use different validation set, including SQuAD, ARC-E, LAMBADA, and PIQA, to conduct the bilevel data training, then compare the corresponding downstream performance.

As shown in Figure 5, our algorithm outperforms random selection on most downstream tasks, except BoolQ, regardless of the validation dataset. Notably, LAMBADA yields the highest average accuracy, improving 1.15% over random selection, likely due to its broad domain coverage.

We also notice that our averaged performance is greatly affected by the accuracy of BoolQ task across all validation datasets. This indicates that it is hard to learn when the answer is too short like yes or no.

D ADDITIONAL RESULTS

Since we use the same experimental settings as MATES(Yu et al., 2024), including pretraining model, data and training steps, we evaluate MATES on the downstream tasks with their checkpoint model (<https://huggingface.co/yuzc19/pythia-410m-mates/blob/main/iter-200800-ckpt.pth>) of 50k steps. For other baselines, we quote Table 1 from MATES(Yu et al., 2024) for convenience of look-up for the performance of more algorithms.

918 Table 8: Results of Different Methods under the 410M/1B Setting. Subscripts denote standard
 919 deviations. Best scores are in bold.
 920

921 Methods(#FLOPs* $1e19$)	922 SciQ	923 ARC-E	924 ARC-C	925 LogiQA	926 OBQA	927 BoolQ	928 HellaSwag	929 PIQA	930 WinoGrande	931 Average
932 410M Setting: 410M model, 25B tokens										
933 Random(6.35)										
934 DSIR(6.35)	64.1(1.5)	40.2(1.0)	25.6 (1.3)	24.7(1.7)	29.4(2.0)	58.9(0.9)	39.7(0.5)	67.1(1.1)	50.6(1.4)	44.5(1.3)
935 LESS(246.35)	63.1(1.5)	39.9(1.0)	23.8(1.2)	27.0(1.7)	28.4(2.0)	58.3(0.9)	39.6(0.5)	66.8(1.1)	51.5(1.4)	44.3(1.3)
936 SemDeDup(7.81)	64.6(1.5)	42.3(1.0)	23.1(1.2)	25.2(1.7)	30.4(2.1)	55.6(0.9)	41.9 (0.5)	67.2(1.1)	51.0(1.4)	44.6(1.4)
937 DsDm(10.72)	63.5(1.5)	42.4 (1.0)	24.4(1.3)	27.6 (1.7)	30.0(2.1)	58.2(0.9)	40.8(0.5)	67.8(1.1)	52.3(1.4)	45.2(1.3)
938 QuRating(26.35)	65.4(1.5)	41.7(1.0)	24.7(1.3)	27.5(1.8)	29.0(2.1)	57.5(0.9)	40.3(0.5)	67.1(1.1)	50.1(1.4)	44.9(1.4)
939 MATES(8.11)	64.8(1.5)	42.0(1.0)	25.4(1.3)	25.3(1.7)	30.2(2.1)	58.9(0.9)	40.7(0.5)	67.5(1.1)	52.1(1.4)	45.2(1.4)
940 BLISS(8.08)	65.7(1.5)	41.5(1.0)	25.0(1.3)	26.1(1.7)	30.8 (2.1)	60.6 (0.9)	41.0(0.5)	67.8(1.1)	51.8(1.4)	45.7(1.4)
941	68.1 (1.5)	42.2(1.0)	25.1(1.3)	27.3(1.7)	29.6(2.0)	59.3(0.9)	41.2(0.5)	68.2 (1.1)	52.0 (1.4)	45.9 (1.4)
942 1B Setting: 1B model, 25B tokens										
943 Random(17.67)										
944 DSIR(17.67)	65.8(1.5)	43.7(1.0)	25.6(1.3)	27.5(1.8)	31.8(2.1)	60.2(0.9)	43.8(0.5)	68.9(1.1)	50.7(1.4)	46.4(1.4)
945 SemDeDup(19.13)	65.8(1.5)	42.6(1.0)	24.7(1.3)	28.7 (1.8)	29.2(2.0)	59.7(0.9)	44.2(0.5)	68.3(1.1)	53.2 (1.4)	46.3(1.4)
946 DsDm(22.04)	66.8(1.5)	45.5(1.0)	25.3(1.3)	27.6(1.8)	30.6(2.1)	60.2(0.9)	45.3(0.5)	69.7(1.1)	52.5(1.4)	47.1(1.4)
947 QuRating(37.67)	68.2(1.5)	45.0(1.0)	26.5 (1.3)	26.6(1.7)	29.4(2.0)	59.0(0.9)	44.8(0.5)	68.9(1.1)	51.9(1.4)	46.7(1.3)
948 MATES(19.97)	67.1(1.5)	45.5(1.0)	25.6(1.3)	26.9(1.7)	29.8(2.0)	60.3(0.9)	45.2(0.5)	70.2(1.1)	51.6(1.4)	46.9(1.3)
949 BLISS(8.08)	67.3(1.5)	44.9(1.0)	25.9(1.3)	28.7 (1.8)	32.2(2.1)	60.9 (0.9)	45.3(0.5)	69.5(1.1)	52.4(1.4)	47.5(1.4)
950	69.4 (1.5)	45.7 (1.0)	24.8(1.3)	25.8(1.7)	33.2 (2.1)	59.8(0.9)	47.8 (0.5)	71.6 (1.1)	52.9(1.4)	47.9 (1.3)

937 Table 9: Experimental settings.
 938

939 Hyperparameters	940 Values
<i>941 Pretrain</i>	
942 Data set	C4
943 Tokens	25B
944 Model	Pythia-410M/1B/2.8B, LLaMA-0.5B
945 batch size	512
946 Sequence length	1024
947 Max learning rate	1e-3
<i>948 bilevel optimization</i>	
949 Proxy/Score model	Pythia-31M (for 410M LLM), Pythia-160M (for 1B LLM), LLaMA-134M (for LLaMA-0.5B LLM)
950 γ	1e-2
951 λ	1e-6
952 batch size	16(Pythia-410M, LLaMA-0.5B)/32(Pythia 1B)
953 Proxy/Score model learning rate(η_1/η_3)	1e-5
954 GDLS learning rate(η_2)	1e-2
955 GDLS steps(\hat{K})	3
956 Score model steps	3k(Pythia-410M/1B)/1k(LLaMA-0.5B)
957 Proxy model steps	3k(Pythia-410M/1B)/1k(LLaMA-0.5B)
958 Initialization of score/proxy model	Randomly initialized

952

E EXPERIMENTAL HYPERPARAMETERS

953 Table 9 shows the hyperparameter settings in our experiments. We use cosine learning rate scheduler
 954 in bilevel optimization, WSD(Yu et al., 2024) learning rate scheduler for pretraining and constant
 955 learning rate for GDLS. We use double loop to update the proxy model when employing 1B LLM,
 956 i.e., 5 steps for the lower level update. The experiments run on 8 A6000 GPUs with Distributed Data
 957 Parallel (DDP) strategy.958

F EVOLUTION OF TRAINING AND VALIDATION LOSS

959 In Figure 6(a), 6(b), we visualize the curves training loss pretraining round 2 and 5.
 960961

G DISTRIBUTED SOFTMAX TO COMPUTE INFLUENCE SCORE

962 In bilevel optimization, the importance weight P_i is computed based on a mini batch that is distributed
 963 across different GPUs. However, back propagation through different GPUs is not implemented by
 964 Pytorch. Thus we deploy "distributed softmax" in practice. In detail, our implementation requires 3

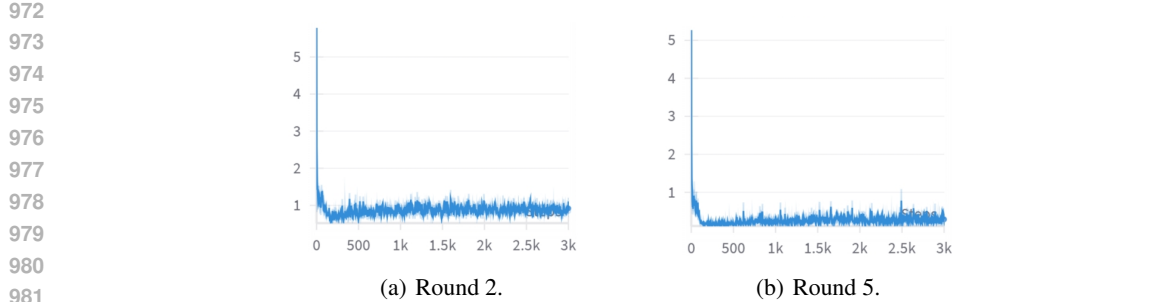


Figure 6: The evolution of training loss in a round.

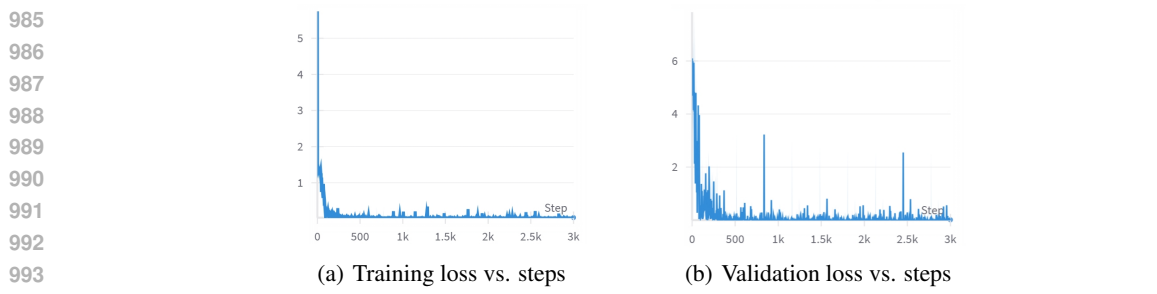


Figure 7: The visualization of lower-level training loss and the upper-level validation loss in round 2 bilevel optimization without KL divergence.

times of communication among GPUs.

$$P_i = \frac{e^{h(\theta_s; \xi_i)}}{\sum_{j=1}^B e^{h(\theta_s; \xi_j)}} \quad (6)$$

As equation (6) shows, the denominator of P_i is the summation of every sample's exponential score. Therefore, in the first communication, each GPU gets the scores from others and calculates the denominator locally. A second communication is required to compute the term $\sum_{j=1}^B P_j \nabla_{\theta_s} h(\theta_s^t; \xi_j)$ in equation (5). In detail, we need to gather gradients of h and \mathcal{L}' of every sample across all GPUs. After computing hyper-gradients of every sample, they are accumulated to update upper-level variables. With efficient communication API provided by Fabric <https://lightning.ai/docs/fabric/stable/>, the time consumed in bilevel optimization of each round is within 1.5 hours.

H RUNNING TIME AND MEMORY

We measured the memory and runtime of the data selection stage for both BLISS and MATES under different target (or pretraining) model sizes (for short, T: target). The results are shown in Table 10. We have two observations:

- BLISS scales well with larger target models. Note that the target model is not an optimization variable for the bilevel optimization and it is only used for calculating the KL divergence. Therefore, it does not affect the scalability of bilevel optimization. When increasing the target from 410M to 1B, BLISS's memory and runtime grow moderately (49.46 → 74.51 GB; 5.03 → 11.82 hours), as expected.
- BLISS is significantly faster than MATES. MATES incurs high cost because each round requires oracle data collection. For every example, MATES performs a one-step gradient update on the target model and evaluates the validation loss change to compute influence scores. This per-example simulation dominates runtime. In contrast, BLISS avoids all

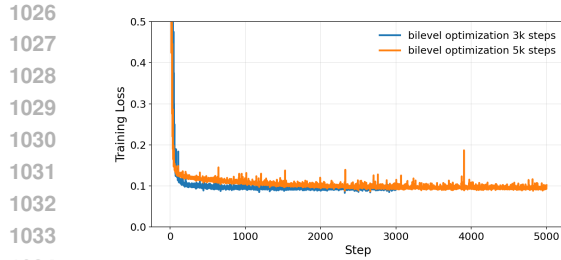


Figure 8: Training loss with different steps.

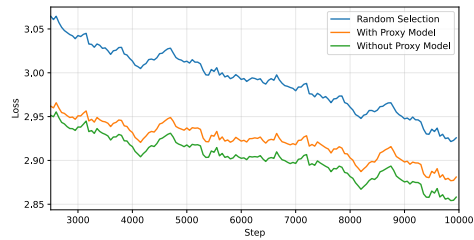


Figure 9: Test loss on SlimPajama-6B.

per-example oracle evaluations in MATES and performs bilevel optimization directly on the proxy/score model, leading to $2 - 3 \times$ faster data selection.

Table 10: The comparison of runtime and memory in data selection stage.

Setting	Memory peak (GB)	Total data selection time (hours)
MATES: T: 410M	36.36	18.0
MATES: T: 1B	63.52	30.32
BLISS: T: 410M	49.46	5.03
BLISS: T: 1B	74.51	11.82

I ABLATION STUDY FOR BILEVEL OPTIMIZATION STEPS

We did the ablation study to investigate the steps of bilevel optimization. As shown in Figure 8, both the 3k-step and 5k-step settings converge to nearly the same training loss. This indicates that 3k steps are sufficient for the proxy model, as increasing the steps to 5k does not yield additional improvements. So we fix the training steps of bilevel optimization to 3k steps in main experiments.

J DOMAIN REWEIGHTING

To verify the fidelity of proxy models to full-scale LLMs, we conduct a domain-reweighting experiment on the SlimPajama-6B dataset (DKYoon, 2023), which contains $d = 7$ domains: ArXiv, Books, C4, CommonCrawl, GitHub, StackExchange, and Wikipedia. The objective is to learn optimal domain weights $\alpha \in \mathbb{R}^d$ such that a model trained on data sampled according to the weights achieves the best downstream performance.

We compare two settings:

1. **Case 1 (with proxy model):** The lower level optimizes a lightweight proxy model (LLaMA-134M) with output alignment to the target LLM (LLaMA-300M), and the upper level learns the domain weights $\tilde{\alpha}$.
2. **Case 2 (without proxy model):** The lower level directly optimizes the target LLM (LLaMA-300M), and the upper level learns the domain weights α .

We perform bilevel optimization for 1,000 steps in both cases to learn the domain weights, where 10% of the original training set is held out as the validation set for the upper-level objective, and the remaining 90% is used as the lower-level training set. After obtaining $\tilde{\alpha}$ and α , we train two final LLaMA-300M models on data sampled according to each set of weights, respectively. Figure 10 presents the learning curves of domain weights for both cases. We observe that the trajectories of $\tilde{\alpha}$ and α are highly similar across most domains (e.g., in the domain of Wikipedia, Book, Stackexchange), demonstrating that the proxy model maintains high fidelity to the full-scale LLM in data selection.

Finally, we evaluate the resulting pretrained LLMs on the test set of SlimPajama-6B, and the results are shown in Figure 9. The test loss curves show that data selection based on the proxy model maintains high fidelity to the full-scale LLM, while significantly outperforming random selection.

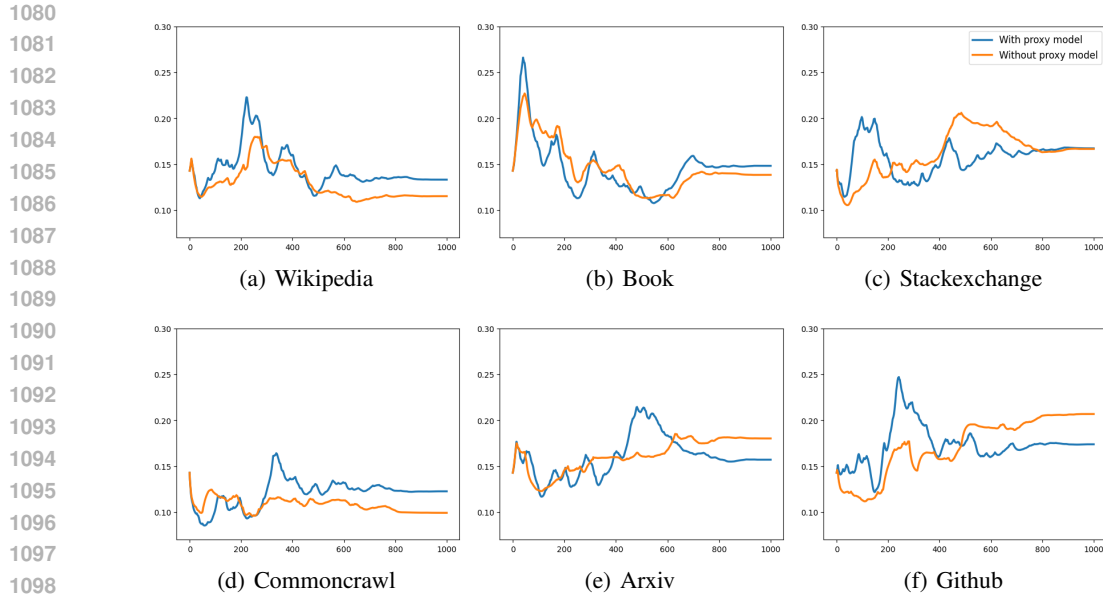


Figure 10: Learning curves of domain weights.

K THE USE OF LARGE LANGUAGE MODELS (LLMs)

LLMs are not involved in our research methodology. Their use is limited to polish the writing.